PHYSICAL REVIEW B VOLUME 50, NUMBER 7 15 AUGUST 1994-I

Wave functions and Fermi surfaces of strongly coupled two-dimensional electron gases investigated by in-plane magnetoresistance

A. Kurobe
Toshiba Cambridge Research Centre, 260 Cambridge Science Park, Milton Road, Cambridge CB4 4WE, United Kingdom

I. M. Castleton, E. H. Linfield, M. P. Grimshaw, K. M. Brown, and D. A. Ritchie
Cavendish Laboratory, Madingley Road, Cambridge CB3 0HE, United Kingdom

M. Pepper
Toshiba Cambridge Research Centre, 260 Cambridge Science Park, Milton Road, Cambridge CB4 4WE, United Kingdom and Cavendish Laboratory, Madingley Road, Cambridge CB3 0HE, United Kingdom

G. A. C. Jones
Cavendish Laboratory, Madingley Road, Cambridge CB3 0HE, United Kingdom
(Received 11 April 1994)

We have studied the in-plane magnetoresistance of coupled double-quantum-well structures, in which each well has a different mobility and where the values of carrier concentration can be varied independently. Resistance resonances, observed at zero magnetic field, were suppressed with an in-plane magnetic field of 1 T, provided the field was perpendicular to the current. The magnetoresistance showed structure which changed systematically with front-gate and back-gate voltages, and was due to the deformation of both wave functions and Fermi surfaces in the in-plane magnetic field.

In recent years there has been much interest in closely separated double two-dimensional electron-gas (2DEG) systems with several effects being observed, such as resonant tunneling between parallel 2DEG's,[1,2] which has been measured in devices where each 2DEG was independently contacted.[3] The Coulomb barrier to tunneling in a high transverse magnetic field has also been reported.[4] If the coupling between the two electron gases becomes large enough, the system at resonance can be described by symmetric and antisymmetric states, which are responsible for lateral transport. When the two 2DEG's possess different values of mobility, an increase in resistance at resonance is then observed.[5,6] This is because a higher mobility 2DEG, which is localized in one of the two wells, extends into both 2DEG's by hybridization at resonance, and thus suffers increased scattering. The symmetric-antisymmetric gap, however, can be destroyed in a strong transverse magnetic field by electron correlation.[7–10]

The requirements of conservation of energy and transverse momentum mean that tunneling between parallel 2DEG's is possible only when the dispersion curves for the two 2DEG's overlap, i.e., only at resonance in the absence of a magnetic field. However, application of an in-plane magnetic field B_{in} shifts the transverse momentum by an amount proportional to B_{in}, and tunneling is only allowed at points where two Fermi circles intersect each other.[11–13] The distortion of the Fermi surfaces in coupled 2DEG's due to in-plane magnetic fields has been measured from Shubnikov–de Haas oscillations,[14] but the in-plane magnetoresistance was not discussed. In this Brief Report we present electron transport results in strongly coupled 2DEG structures in an in-plane magnetic field. The measured lateral transport is due to symmetric and antisymmetric states, which is in sharp contrast to the tunnel resistance measurements reported in Ref. 11. We show that the resonance resistance is suppressed by an in-plane magnetic field of about 1 T, and the degree of the suppression depends on the direction of the in-plane field relative to the current. We also found structure at a high magnetic field, which moved with front- and back-gate voltages. These effects are discussed as being associated with the deformation of wave functions and the Fermi surfaces in the in-plane magnetic field.

The sample employed here is a modulation-doped double-quantum-well (DQW) structure grown on a semi-insulating GaAs substrate by molecular-beam epitaxy (MBE). The DQW consists of two 150-Å-wide quantum wells separated by a 25-Å $Al_{0.33}Ga_{0.67}As$ barrier. Electrons in the 2DEG's were supplied by Si-doped $Al_{0.33}Ga_{0.67}As$ layers (200 Å wide, 1×10^{18} cm^{-3}) placed above and below the DQW structure; for the lower layer a 400-Å $Al_{0.33}Ga_{0.67}As$ spacer separated the doped $Al_{0.33}Ga_{0.67}As$ from the DQW, while for the top layer a 200-Å spacer was used. The whole of the DQW structure was isolated by a 0.31-μm $Al_{0.33}Ga_{0.67}As$ barrier from an n^+ GaAs back-gate layer grown underneath. The growth temperature T_g was 630° except at the back n^+ $Al_{0.33}Ga_{0.67}As$ layer, where T_g was lowered to 520 °C. Ohmic contacts to the double 2DEG's were, however, required without contacting to the n^+ GaAs back-gate layer, and this was achieved using MBE regrowth on an *in situ* focused ion beam patterned epilayer.[15] After growth, devices were processed with a Hall bar geometry with a front Schottky gate as well as a back gate. The mobility of the front 2DEG at $T=1.5$ K was 2.0×10^5 $cm^2/V\,s$ at

 ©1994 The American Physical Society

the carrier concentration of 1.2×10^{11} cm^{-2}, while that of the back 2DEG was 1.1×10^{5} cm^2/V s at the same carrier concentration; this was obtained by fully depleting one of the 2DEG's. The somewhat lower mobility in the back 2DEG was due to diffusion of dopant from the doped $Al_{0.33}Ga_{0.67}As$ layer into the back $Al_{0.33}Ga_{0.67}As$ spacer during growth.

The resistance as a function of front-gate voltage (V_{fg}) at various back-gate voltages (V_{bg}) is shown by solid curves in Fig. 1. Arrows indicate the position of the resonance, which was determined from the beating of the Shubnikov–de Haas (SdH) oscillations at $T=1.5$ K.[14] The symmetric-antisymmetric energy gap of $\Delta_{SAS}=1.2\pm0.1$ meV, which is in agreement with a theoretical value of 1.3 meV, was also obtained from SdH oscillations. A resonant increase in resistance, i.e., resistance resonance, can be seen in Fig. 1(a) at the right-hand side of the actual resonance voltage, because the resistance peak is distorted due to the change of the front 2DEG mobility with the front-gate voltage. A mobility ratio estimated from the size of the resistance resonance[5] was 2, which is comparable to 1.8, the value derived from the mobility measurements.

We applied a magnetic field parallel (to within 0.2°) to the 2DEG's. When the in-plane magnetic field B_{in} was applied perpendicular to the source-drain current j, the resistance resonance was suppressed at a magnetic field as low as 1 T [broken curves in Fig. 1(a)]. We also observed anisotropy in the effect of an in-plane field [Fig. 1(b)], as an in-plane magnetic field parallel to the current also diminished the peak, not by the suppression of the resistance resonance but by enhancement of the resistance away from the resonance.

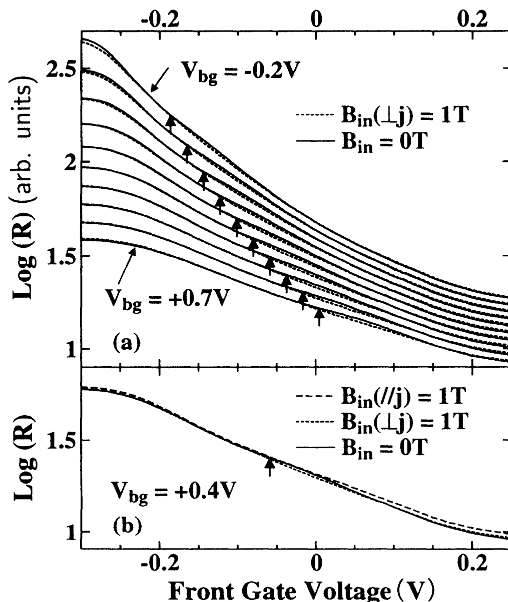

FIG. 1. Resistance resonance as a function of front-gate voltage with and without an in-plane magnetic field at $T=4.2$ K. Arrows indicate resonance front-gate voltage. (a) $B_{in}\perp j$. Back-gate voltage V_{bg} was changed from -0.2 to $+0.7$ V with a step of 0.1 V. Curves are shifted for clarity. The systematic change in the front-gate voltage required for resonance as a function of back-gate voltage confirms that the carrier concentration in each well is well controlled by the gates. (b) Anisotropy of the in-plane magnetoresistance. $V_{bg}=+0.4$ V.

The suppression of the resistance resonance by an in-plane magnetic field was observed more clearly in a different sample, in which the mobility ratio was increased to ≈14, the mobility of the back 2DEG being $\approx2\times10^4$ cm^2/V s. For this device the back n^+ $Al_{0.33}Ga_{0.67}As$ layer was grown at a higher temperature of 580 °C to enhance diffusion of the dopant. The resistance as a function of the back-gate voltage, in this case, is plotted in Fig. 2 for $V_{fg}=-0.15$ V at various in-plane magnetic fields. When the in-plane magnetic field was applied perpendicular to the current, the resistance resonance was fully suppressed at the field of 1 T. On the other hand, the suppression was not complete if the field was parallel to the current.

These experimental results can be understood from the shape of the wave function in an in-plane magnetic field. Let us consider a DQW Hamiltonian in a magnetic field $\mathbf{B}=(0,B_{in},0)$ in the xy plane.[14,16,17] Taking a Landau gauge, $\mathbf{A}=(zB_{in},0,0)$, the Hamiltonian reads

$$H=\frac{\hbar^2}{2m}\left[k_x+\frac{eB_{in}z}{\hbar}\right]^2+\frac{\hbar^2k_y^2}{2m}-\frac{\hbar^2}{2m}\frac{\partial^2}{\partial z^2}+V(z)\ , \quad (1)$$

where $V(z)$ is the DQW confining potential, and k_x and k_y are wave vectors in the x and y directions, respectively. At $B_{in}=0$ an interwell coupling lifts degeneracy at resonance, and symmetric $|\varphi_S\rangle$ and antisymmetric states $|\varphi_{AS}\rangle$ are formed. Those low mobility delocalized states show parabolic k_x dispersions (each minimum at $k_x=0$), and the shape of the wave functions in the z direction is independent of k_x. Once B_{in} is finite, however, the first term in Eq. (1) shifts the parabolic k_x dispersions for states localized in each well by an amount $\Delta k_x=\pm ez_{SAS}B_{in}/\hbar$, where $z_{SAS}=\langle\varphi_{AS}|z|\varphi_S\rangle$. This is illustrated in the right inset of Fig. 2 for $k_y=0$. The interwell coupling, in this case, hybridizes localized QW or-

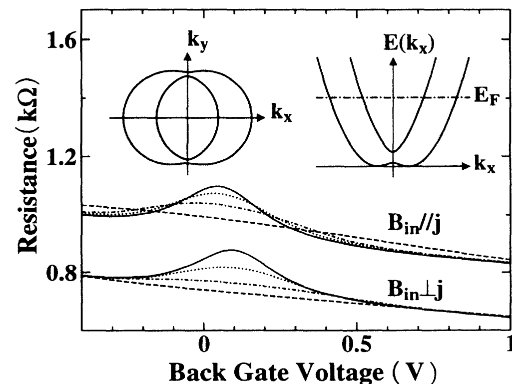

FIG. 2. Suppression of resistance resonance by in-plane magnetic fields for a device with a mobility ratio ≈14. $T=4.2$ K. Data for $B_{in}\|j$ are shifted for clarity. $B_{in}=0$ T (solid curves), 0.2 T (dotted curves), 0.4 T (broken dotted curves), and 1 T (broken curves). Insets show dispersion curves (right) and Fermi surfaces (left) for a coupled DQW structure in an in-plane magnetic field.

bits only near $k_x=0$, where the two shifted parabolic dispersions cross each other. Therefore, if B_{in} is large enough, the wave functions at the Fermi level are decoupled and localized by the in-plane magnetic field. This can lead to the suppression of the resistance resonance.

The anisotropy of the in-plane magnetoresistance is explained by the hybridization of wave functions on the Fermi surfaces. As is shown in the left inset of Fig. 2, the Fermi surfaces arise from two shifted Fermi circles originating from quantum wells. But they are distorted where the two circles overlap each other, and the interwell coupling hybridizes wave functions to form delocalized states. When the current is driven perpendicularly to the magnetic field, i.e., in the x direction, contributions to the conductivity come mainly from the Fermi surfaces near the k_x axis.[18] Since these states are easily decoupled and localized by the in-plane magnetic field, the resistance resonance is suppressed. On the other hand, if the current is applied along the y axis, i.e., parallel to the magnetic field, the contribution from those near the k_y axis will be larger. This leads to less suppression of the resistance resonance, since states in those regions of the Fermi surfaces are hybridized even in the presence of an in-plane magnetic field.

Further experimental investigations were made for the device with a lower mobility ratio, because both of the 2DEG's showed large mobility, and the carrier concentration in each well was determined from the SdH oscillation. Figure 3 shows the negative magnetoresistance ($B_{in} \perp j$) due to the suppression of the resistance resonance at $V_{bg}=0$ V when the front-gate voltage was adjusted to resonance (solid curve) and was away from the resonance (broken curve). We defined a decay magnetic field B_{decay}, at which the in-plane magnetoresistance at resonance condition falls off by half, and measured B_{decay} at various back-gate voltages, i.e., different carrier concentrations. B_{decay} was found to decrease almost linearly with the Fermi wave vector k_F (inset of Fig. 3). Here $k_F(=\sqrt{2\pi n_s})$ was calculated using the carrier concentration n_s in each well at resonance. As a lower Fermi level implies a smaller wave vector (see the right inset of Fig. 2), the hybridization is stronger and the suppression of the resistance resonance occurs at a larger magnetic field. It is further noted that the hybridization away from the resonance is not maximized at $B_{in}=0$ T, resulting in an increase in hybridization by an in-plane magnetic field at one side of the Fermi surfaces (see top left inset of Fig. 4). This explains why the decay magnetic field is minimized at the resonance.

The in-plane magnetoresistance measurements were extended to higher fields to probe the distortion of the Fermi surfaces. Figure 4 shows the results at $V_{bg}=+0.4$ V for a range of front-gate voltages. The carrier concentration in the back well was 3.02×10^{11} cm^{-2}, the resonance front-gate voltage was -0.06 V, and the in-plane magnetic field was parallel to the current. A steplike increase in the resistance was observed below 2 T, the field at which this occurred increased as the front-gate voltage moved away from the resonance. Increasing the field resulted in a dip followed by an increase. The location of the dip decreased in magnetic field as the front-gate voltage was made more negative. Similar behavior was also observed when B_{in} was perpendicular to the current.

An in-plane magnetic field B_0, at which one of the Fermi circles is inscribed by the other, was calculated from the carrier densities in the front and back wells, and is shown in Fig. 4 for each front-gate voltage. The position of B_0 coincides with that of the steplike increase of the resistance at a lower magnetic field, and suggests that it is due to increased hybridization at one side of the Fermi surfaces ("in-plane magnetic-field-induced resistance resonance").

In order to understand the dip in Fig. 4, we calculated the shape of the Fermi surfaces as a function of B_{in}. We first solved Schrödinger and Poisson equations self-consistently to reproduce observed carrier concentrations, and obtained wave functions numerically at $B_{in}=0$ T. Using these as basis functions, the Hamiltonian (1)

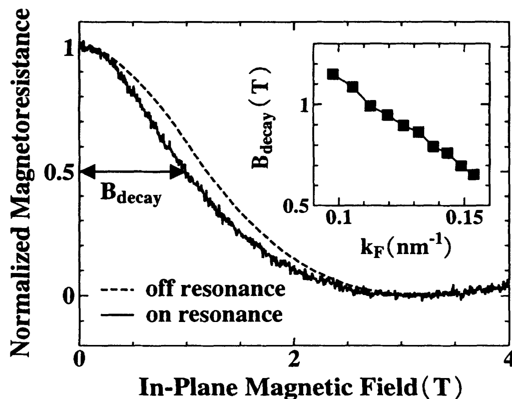

FIG. 3. Negative in-plane magnetoresistance ($B_{in} \perp j$) at and away from the resonance front-gate voltage. $V_{bg}=0$ V, $T=4.2$ K. Solid curve: $V_{fg}=-0.12$ V. Broken curve: $V_{fg}=-0.04$ V. Definition of B_{decay} is also shown. Inset shows B_{decay} as a function of the Fermi wave vector.

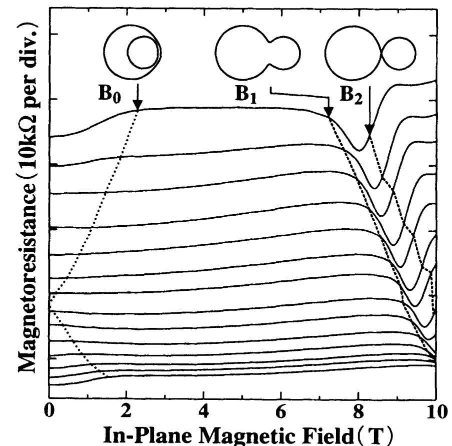

FIG. 4. In-plane magnetoresistance ($B_{in} \parallel j$) at various front-gate voltages. $V_{bg}=+0.4$ V, $T=4.2$ K. V_{fg} was changed from -0.225 V (top curve) to $+0.1$ V (bottom curve) with a step of 25 mV. Curves are shifted for clarity. Broken lines connect calculated in-plane fields B_0, B_1, and B_2 at each front-gate voltage, corresponding Fermi surfaces being illustrated in insets.

was diagonalized, and magnetic fields B_1 and B_2 in Fig. 4 were obtained at each front-gate voltage. If the in-plane field is large enough, the two Fermi circles separate from each other at B_2. Before this, however, at a magnetic field B_1, the upper dispersion branch in Fig. 2 is depopulated, i.e., the inner Fermi surface in Fig. 2 disappears. As is shown in Fig. 4, the resistance dip always resides between B_1 and B_2, i.e., the resistance decreases when the Fermi level lies between the gap created by the interwell coupling. This strongly suggests that the origin of the dip is the suppression of the intersubband scattering between the lower and upper dispersion branches. Unlike the case of multisubbands in a single channel,[19,20] the resistance increases again, because two enclosed Fermi surfaces are restored due to the double-well shape of the lower dispersion branch.

In conclusion, we have demonstrated that the in-plane magnetoresistance characterizes wave-function coupling and Fermi-surface distortion in strongly coupled 2DEG systems.

Work at the Cavendish Laboratory was supported by the U.K. Science and Engineering Research Council. D.A.R. acknowledges the support of the Toshiba Cambridge Research Centre.

[1]J. P. Eisenstein, L. N. Pfeiffer, and K. W. West, Appl. Phys. Lett. **58**, 1497 (1991).

[2]W. Demmerle, J. Smoliner, G. Berthold, E. Gornik, G. Weimann, and W. Schlapp, Phys. Rev. B **44**, 3090 (1991).

[3]J. P. Eisenstein, L. N. Pfeiffer, and K. W. West, Appl. Phys. Lett. **57**, 2324 (1990).

[4]J. P. Eisenstein, L. N. Pfeiffer, and K. W. West, Phys. Rev. Lett. **69**, 3804 (1992).

[5]A. Palevski, F. Beltram, F. Capasso, L. Pfeiffer, and K. W. West, Phys. Rev. Lett. **65**, 1929 (1990).

[6]Y. Ohno, M. Tsuchiya, and H. Sakaki, Appl. Phys. Lett. **62**, 1952 (1993).

[7]G. S. Boebinger, H. W. Jiang, L. N. Pfeiffer, and K. W. West, Phys. Rev. Lett. **64**, 1793 (1990).

[8]Y. W. Suen, J. Jo, M. B. Santos, L. W. Engel, S. W. Hwang, and M. Shayegan, Phys. Rev. B **44**, 5947 (1991).

[9]G. S. Boebinger, L. N. Pfeiffer, and K. W. West, Phys. Rev. B **45**, 11 391 (1992).

[10]A. H. MacDonald, P. M. Platzman, and G. S. Boebinger, Phys. Rev. Lett. **65**, 775 (1990).

[11]J. P. Eisenstein, T. J. Gramila, L. N. Pfeiffer, and K. W. West, Phys. Rev. B **44**, 6511 (1991).

[12]J. A. Simmons, S. K. Lyo, J. F. Klem, M. E. Sherwin, and J. R. Wendth, Phys. Rev. B **47**, 15 741 (1993).

[13]L. Zheng and A. H. MacDonald, Phys. Rev. B **47**, 10 619 (1993).

[14]G. S. Boebinger, A. Passner, L. N. Pfeiffer, and K. W. West, Phys. Rev. B **43**, 12 673 (1991).

[15]E. H. Linfield, G. A. C. Jones, D. A. Ritchie, and J. H. Thompson, Semicond. Sci. Technol. **8**, 415 (1993).

[16]J. M. Heisz and E. Zarembra, Semicond. Sci. Technol. **8**, 575 (1993).

[17]T. Jungwirth and L. Smrcka, J. Phys. Condens. Matter **5**, L217 (1993).

[18]Note that if a wave vector **k** is on the Fermi surface, the velocity of an electron $v(\mathbf{k})=\hbar^{-1}(\partial E/\partial \mathbf{k})$ is normal to the Fermi surface. Since the x component of the velocity contributes to the conduction in the x direction, the conductivity can be evaluated mainly from the Fermi surface near the k_x axis in the left inset of Fig. 2.

[19]T. Englert, J. C. Maan, D. C. Tsui, and A. C. Gossard, Solid State Commun. **45**, 989 (1983).

[20]S. Mori and T. Ando, J. Phys. Soc. Jpn. **48**, 865 (1980).